arXiv:0806.3453v1 [cond-mat.supr-con] 20 Jun 2008

The Fermi surface of $Ba_{1-x}K_xFe_2As_2$ and its evolution with doping

C. Liu,[1] G. D. Samolyuk,[1] Y. Lee,[1] N. Ni,[1] T. Kondo,[1] A. F. Santander-Syro,[2,3] S. L. Bud'ko,[1] J. L. McChesney,[4] E. Rotenberg,[4] T. Valla,[5] A. V. Fedorov,[4] P. C. Canfield,[1] B. N. Harmon,[1] and A. Kaminski[1]

[1]*Ames Laboratory and Department of Physics and Astronomy, Iowa State University, Ames, Iowa 50011, USA*
[2]*Laboratoire Photons Et Matière, UPR-5 CNRS, ESPCI, 10 rue Vauquelin, 75231 Paris cedex 5, France*
[3]*Labratoire de Physique des Solides, UMR-8502 CNRS, Université Paris-Sud, Bât. 510, 91405 Orsay, France*
[4]*Advanced Light Source, Berkeley National Laboratory, Berkeley, California 94720, USA*
[5]*Condensed Matter Physics and Materials Science Dept., Brookhaven National Laboratory, Upton, New York 11973, USA*

(Dated: August 10, 2021)

We use angle-resolved photoemission spectroscopy (ARPES) to investigate the electronic properties of the newly discovered iron-arsenic superconductor, $Ba_{1-x}K_xFe_2As_2$ and non-supercondcuting $BaFe_2As_2$. Our study indicates that the Fermi surface of the undoped, parent compound $BaFe_2As_2$ consists of hole pocket(s) at Γ (0,0) and larger electron pocket(s) at X (1,0), in general agreement with full-potential linearized plane wave (FLAPW) calculations. Upon doping with potassium, the hole pocket expands and the electron pocket becomes smaller with its bottom approaching the chemical potential. Such an evolution of the Fermi surface is consistent with hole doping within a rigid band shift model. Our results also indicate that FLAPW calculation is a reasonable approach for modeling the electronic properties of both undoped and K-doped iron arsenites.

PACS numbers: 79.60.-i, 74.25.Jb, 74.70.-b

Iron-Arsenic based materials comprise a very interesting class of materials with many unusual properties. For example, they have recently been shown to be superconducting with a T_c as high as 55K[1, 2, 3]. This discovery has initiated a frenzy of research activity, which until very recently was limited to studies of only polycrystalline samples. Initial experiments focused on fluorine-doped rare earth oxide based materials (RFeAsOF) [4, 5, 6]. To date, there is very little photoemission data available on these compounds[7, 8, 9] with only one angle resolved study[10]. The recent discovery of superconductivity in oxygen free $Ba_{1-x}K_xFe_2As_2$ [11] suggests that the superconductivity is ultimately linked to the electronic properties of the iron arsenic layer(s) with the remaining layers acting as a charge reservoir. This scheme closely resembles the situation found in the cuprates but without oxygen. In both $BaFe_2As_2$ and $SrFe_2As_2$ there are clear structural phase transitions from a high temperature tetragonal to low temperature orthorhombic phases.[12, 13] When potassium is substituted for barium, the temperature at which the structural transition occurs is suppressed and superconductivity emerges[11, 12]. Some experiments also point to the existence of a transition into a spin density wave (SDW) state at higher temperature [5, 14] and related changes of the electronic structure[15]. Determining the effects of doping on low lying electronic excitations is essential for this study, as they play significant role in determining the normal state and superconducting properties. It is equally important to understand the electronic properties of the parent compound because undoped systems are easier to model theoretically and they represent a basis for higher order approximations. The information about electronic structure and its evolution with doping is deemed essential to formulate a successful model of superconductivity in these fascinating systems.

The recent growth of large, high quality single crystals [12] has opened up the possibility of examining the electronic properties of these materials. Here we present data from angle resolved photoemission spectroscopy (ARPES) on the Fermi surface and band dispersion, and discuss how they are affected by doping with potassium. We find in the undoped samples, the Fermi surface consists of a smaller hole pocket centered at Γ (0,0,0) and a larger electron pocket located at each of the X points. Upon doping with potassium, the Γ hole pocket increases in size and the X pocket contracts. There are also significant shifts in energy for lower lying, fully occupied bands. In potassium doped system - on the verge of superconductivity the bottom of X band is located in close proximity to the chemical potential. This may have significance for the emergence of the superconductivity in this system. Our experimental results are in general agreement with band calculations for both undoped and doped system.

Single crystals of the parent compound, $BaFe_2As_2$, and potassium doped samples, $Ba_{1-x}K_xFe_2As_2$, with an approximate doping $x = 0.45$ were grown out of a Sn flux using conventional high temperature solution growth techniques[12]. Large (up to 2×2 mm) single crystals were cleaved *in situ* yielding flat mirror-like surfaces. The experimental data was acquired using a laboratory-based ARPES system consisting of a Scienta SES2002 electron analyzer, GammaData UV lamp and custom de-

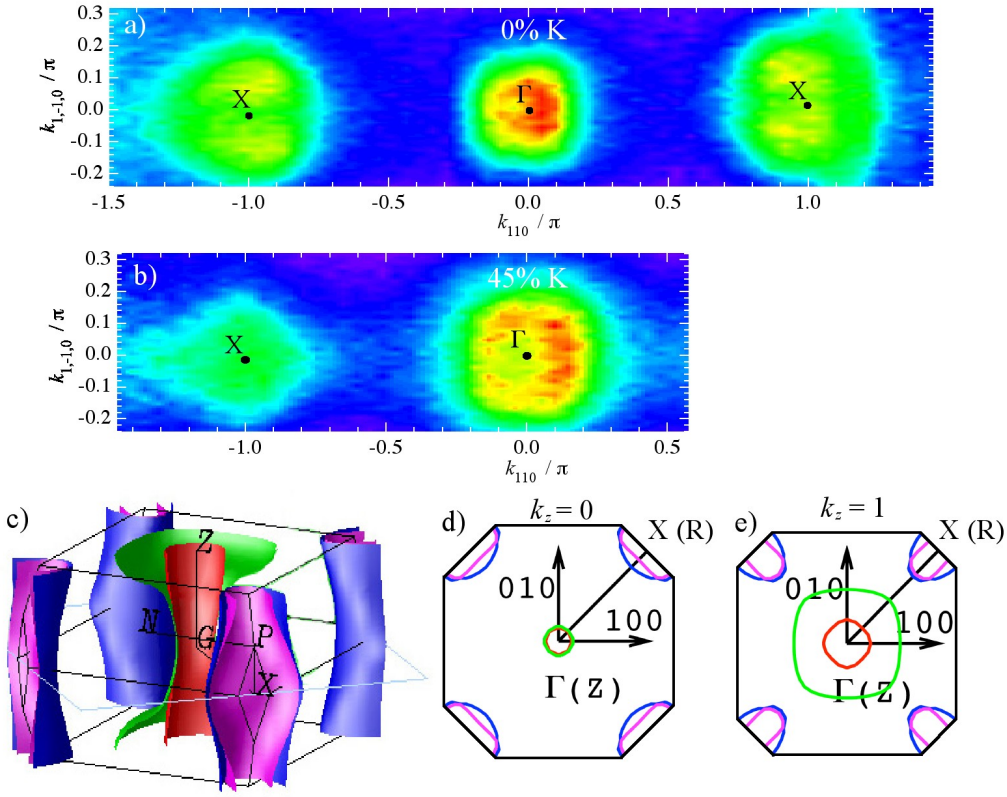

FIG. 1: (color online) Measured Fermi surface (FS) of $BaFe_2As_2$ and $Ba_{1-x}K_xFe_2As_2$ and calculated FS for undoped case. a) FS map of $BaFe_2As_2$ - intensity of the photoelectrons integrated over 20 meV about the chemical potential obtained with 40.8 eV photons. Experiment was done at $T = 100$K. Areas of bright color mark the locations of the FS. b) FS map of $Ba_{1-x}K_xFe_2As_2$ with nominal $x = 0.45$ measured under the same conditions as (a). c) 3-dimensional FS of $BaFe_2As_2$ obtained from FLAPW calculations. d) FS cross-section for $k_z = 0$ (X-Γ plane) obtained by FLAPW calculations. e) same as (d) but for $k_z = 1$ (R-Z plane).

signed refocusing optics. The samples were cooled using a closed-cycle refrigerator. Measurements were performed on several samples and all yielded similar results for the band dispersion and Fermi surface. All data were acquired using the HeII line with a photon energy of 40.8 eV. The momentum resolution was set at 0.014 $Å^{-1}$ and 0.06 $Å^{-1}$ parallel and perpendicular to the slit direction. The energy resolution was 30 meV for the Fermi surface scans and 15 meV for the intensity maps. Our full-potential linearized plane wave (FLAPW) calculation [18] have done with local density approximation(LDA) [19] , and the experimental lattice constants [11] for the undoped parent compound $BaFe_2As_2$ and potassium doped $Ba_{1-x}K_xFe_2As_2$ with $x = 0.4$. Total energy minimization was used to determine $z_{As} = 0.341$c.

The shape of the Fermi surface (FS) is normally illustrated by plotting the photoelectron intensity at the chemical potential[16, 17]. In Fig. 1a and b we plot this quantity integrated within 20 meV energy range for undoped and potassium-doped samples. The Fermi surface of undoped $BaFe_2As_2$ consists of a smaller circular-shaped hole pocket centered at Γ and larger electron pockets at X points with also a circular shape, whose spectrum at two corners in the $k_{1,-1,0}$ direction is somewhat more intense. In the potassium doped samples (Fig. 1b) the Γ pocket becomes larger and the X pocket shrinks, which is consistent with hole doping of carriers. We note that the X-pockets in doped samples have a characteristic "starrish" shape, in reasonable agreement with FLAPW calculations shown in Figs. 1c-e. The variation of intensity around each contour of both Γ and X pockets is due to photoemission matrix elements.

In Fig. 2 we show how the shape of both the Γ and X bands evolves with binding energy and potassium doping. With increasing binding energy, the contour of the Γ pocket becomes larger - consistent with its hole-like topology, while the X pocket becomes smaller - consistent with its electron-like topology. One notable fact shown in Fig. 2 is that the size of the pockets at a binding energy 0.04eV in the parent compound is similar to that of the potassium doped compound at the Fermi level. In other words, based on a rigid-band shifting scenario, we

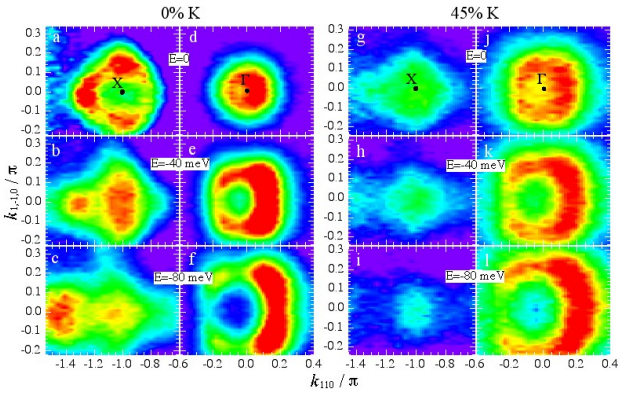

FIG. 2: (color online) Electron intensity map for selected binding energies of the undoped and potassium-doped samples. All data was taken at $T = 100$K. Panels (a)-(f) present the data of undoped $BaFe_2As_2$, while panels (g)-(l) present the data of $Ba_{1-x}K_xFe_2As_2$ with nominal $x = 0.45$. The three rows of panels present the data at the chemical potential E_F, binding energy $E = 0.04$ and 0.08eV, respectively; the two columns of panels for each doping present the intensity map covering a k-space area near the X-point [(a)-(c), (g)-(i)] and the Γ-point [(d)-(f), (j)-(l)], respectively.

could approximately say that the potassium hole doping lowers the chemical potential by ∼40 meV. We note also that with potassium doping the bottom of the X band is located in very close proximity to the chemical potential.

In figure 3 we plot the experimental band dispersion data perpendicular to the Γ-X direction along cuts through the X and Γ points (i.e. along the $k_{1,-1,0}$ direction). For both the $x = 0$ and $x = 0.45$ doping levels, the hole pockets at Γ and the electron pockets at X are shown (see also Fig. 2) and are in general agreement with band calculations. Here we can examine the relative size of the hole pockets and the electron pockets in more detail by studying the Fermi crossing momenta (k_Fs) marked by blue curves in Figs. 3c, 3d, 3h and 3i. These k_Fs were determined from the most intense points in the momentum distribution curves (MDCs) at the Fermi level. The number of k-curves between two k_Fs is proportional to the actual size of each pocket.

The calculated Fermi surface (Fig. 3e) of BaFe2As2 and LaFeAsO compounds are very similar [20, 21]. However, details of the bandstructure around Fermi energy were sensitive to this parameter, as previously reported [22]. With the change of As position from experimental one to the correspondent of energy minima the shape of Fermi surface sheet corresponded to holes pocket, shown by green color on Fig. 1c, changes from cylinder without dispersion along k_z-direction [21] to modulated cylinder with strong dispersion along k_z. The band structure for the doped material performed using virtual crystal method is shown in Fig. 3j. Clearly, in the undoped parent compound both in experimental data as well as calculation the X-pocket is larger than the Γ pocket, whereas in the $x = 0.45$ potassium-doped samples, the opposite is the case. This effect is consistent with the idea of rigid-band shifting, namely, potassium doping lowers the chemical potential of the parent compound, while the shapes of the bands are left unchanged. A second notable doping dependent feature is the energy shift of two fully occupied bands, marked by black arrows in Figs. 3b, 3e, 3g and 3j, where Fig. 3e and 3j plot the calculated band structure of the undoped $BaFe_2As_2$ and potassium-doped $Ba_{1-x}K_xFe_2As_2$ with $x = 0.45$, respectively. These arrows point to similar characteristic features in experimental data and calculations and how they change upon doping. On potassium doping, the upper band shifts to lower binding energy by ∼130 meV, while the lower band shifts to lower binding energy by ∼180 meV. This fact is in qualitative agreement with calculations. A third feature notable in Fig. 3 is the missing of bilayer splitting in the measured data. This fact also agrees well with the FLAPW calculations, where the two bands constructing the Fermi surface are highly degenerated in both the undoped and K-doped systems. All these doping dependent features point to the conclusion that the FLAPW approximation is valid in both undoped and hole-doped iron arsenic superconductors.

Despite the fact that our potassium-doped samples display bulk superconductivity, we did not detect a superconducting gap in the ARPES measurement down to 12K. This may be due to loss of the potassium from the surface in the ultra-high vacuum (UHV) environment or possibly a variation in potassium doping between different layers, which suggests a strong dependence of the critical temperature on doping. Our data also indicates that upon further doping to a point where the material becomes superconducting, the bottom of the X pocket will be in very close proximity to the chemical potential. Such an increase of the density of states (DOS) may be relevant to the emergence of superconductivity in these materials.

In conclusion we have determined the evolution of the Fermi surface and band dispersion for $Ba_{1-x}K_xFe_2As_2$ for $x = 0$ and $x = 0.45$. We find in the undoped samples, the Fermi surface consists of a smaller hole pocket centered at Γ (0,0,0) and a larger electron pocket located at each of X points. This is in general agreement with band calculations. Upon doping, the Γ hole pocket increases in size and the X pocket contracts, which is consistent with hole doping. The conduction bands shift in energy with doping in a similar fashion, in accordance with a rigid band shift scheme. Our data indicates that upon further doping to a point where the material becomes superconducting, the bottom of the X pocket will be in very close proximity to the chemical potential. The consequent increase in the DOS may be relevant for the emergence of superconductivity in these materials.

We are grateful for useful discussions with Jörg Schmalian. We thank Helen Fretwell for useful remarks

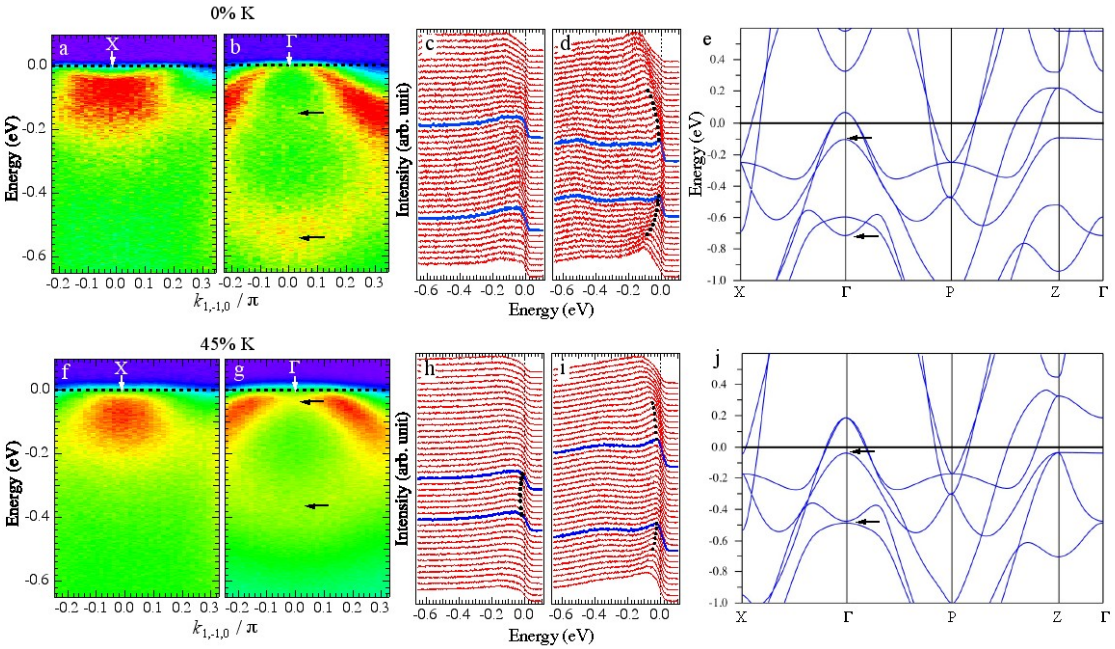

FIG. 3: (color online) Experimental band dispersions and corresponding energy distribution curves (EDCs) along selected cuts, compared with theoretical band structure. Panels (a)-(d) present the data of undoped $BaFe_2As_2$, while panels (e)-(h) present the data of $Ba_{1-x}K_xFe_2As_2$ with nominal $x = 0.45$. a) ARPES intensity map in X region for undoped sample. b) ARPES intensity map in Γ region for undoped sample. c,d) EDC's for same cuts as in (a) and (b). Curves at Fermi momentum are marked blue. e) Results of FLAPW band calculation for parent compound $BaFe_2As_2$. f) ARPES intensity map in X region for doped sample x=0.45. g) ARPES intensity map in Γ region for doped sample x=0.45. h,i) EDC's for same cuts as in (f) and (g). Curves at Fermi momentum are marked blue. e) Results of FLAPW band calculation for doped $Ba_{1-x}K_xFe_2As_2$ with x=0.45.

and corrections. Work at Ames Laboratory was supported by the Department of Energy - Basic Energy Sciences under Contract No. DE-AC02-07CH11358. ALS is operated by the US DOE under Contract No. DE-AC03-76SF00098. Brookhaven National Laboratory is supported by US DOE under Contract No. DE-AC02-98CH10886. AFSS thanks LPEM for financial support.

[1] Yoichi Kamihara, Takumi Watanabe, Masahiro Hirano, and Hideo Hosono, J. Am. Chem. Soc. **130**, 3296 (2008).
[2] Hiroki Takahashi *et al.*, Nature(London) **453**, 376 (2008)
[3] Ren Zhi-An *et al.*, Chin. Phys. Lett. **25**, 2215 (2008).
[4] T. Y. Chen, Z. Tesanovic, R. H. Liu, X. H. Chen and C. L. Chien, /nature07081 (2008)
[5] Clarina de la Cruz *et al.*, Nature **453**, 899(2008)
[6] F. Hunte *et al.*, Nature **453**, 903 (2008),
[7] T. Sato, *et al.*, J. Phys. Soc. Jpn. **25**, in press (2008).
[8] Xiaowen Jia, *et al.*, arXiv:0806.0291, (2008)
[9] Haiyun Liu *et al.*, arXiv:0805.3821, (2008)
[10] C. Liu *et al.*, arXiv:0806.2147, (2008)
[11] M. Rotter, M. Tegel and D. Johrendt, arXiv:0805.4630, (2008)
[12] N. Ni *et al.*, arXiv:0806.1874, (2008)
[13] J. -Q. Yan *et al.*, arXiv:0806.2711, (2008)
[14] X. F. Wang *et al.*, arXiv:0806.2452, (2008)
[15] L. X. Yang *et al.*, arXiv:0806.2627, (2008)
[16] J. Mesot *et al.*, Phys. Rev. B **63**, 224516 (2001)
[17] H. M. Fretwell *et al.*, Phys. Rev. Lett. **84**, 4449 (2000)
[18] P. Blaha, K. Schwarz, G. K. Madsen, D. Kvasnick and J. Luitz, *WIEN2K, An augmented Plane wave + Local Orbitals Program for Calculation Crystal Properties.* (K. Schwarz, TU Wien, Austria, 2001) ISBN 3-9501031-1-2
[19] J. P. Perdew and Y. Wang, Phys. Rev. B45, 13244 (1992)
[20] D.J. Singh and M.-H. Du, arXiv:0803.0429v1 (2008)
[21] I. A. Nekrasov, Z. V. Pchelkina and M. V. Sadovskii, arXiv:0806.2630v2 (2008)
[22] I. I. Mazin, M.D. Johannes, L. Boeri, K. Koepernik and D.J. Singh, arXiv:0806.1869v1 (2008)